Available online at www.sciencedirect.com
SCIENCE DIRECT®
Journal of Photochemistry and Photobiology A: Chemistry 163 (2004) 517–522
Journal of Photochemistry and Photobiology A:Chemistry
www.elsevier.com/locate/jphotochem

Effect of doping mode on the photocatalytic activities of Mo/TiO_2

Ying Yang[1], Xin-jun Li*, Jun-tao Chen, Liang-yan Wang

Guangzhou Institute of Energy Conversion, The Chinese Academy of Sciences, Guangzhou 510640, PR China

Received 16 September 2003; received in revised form 23 December 2003; accepted 13 February 2004

Abstract

The thin films of photocatalyst, TiO_2 doped by Mo^{6+} in different forms, were prepared by sol–gel method. The photocatalysts were characterized by X-ray diffraction (XRD), UV-Vis transmittance spectra and electrochemical impedance spectroscopy, and the photocatalytic activity was characterized by photocatalytic degradation of aqueous methyl orange under UV radiation. The results showed that the TiO_2 doped by Mo^{6+} extend absorption edge and interfacial charge transfer resistance decrease. The photocatalytic activity of TiO_2 doped by Mo^{6+} in bottom is much better than that of pure TiO_2, those doped in surface, or those doped uniformly. The activity of TiO_2 doped by Mo^{6+} in bottom mode at optimal concentration, 1 at.%, increased nearly two times than pure TiO_2. The effects of doping modes on the photocatalytic activities were discussed in the terms of separateness of charge carriers that there maybe form barrier of carrier in bottom doping mode and then restraining the (e^-–h^+) pair recombination.

Keywords: Photocatalysis; Titanium dioxide; Molybdenum; Doping mode; Thin film

1. Introduction

Heterogeneous photocatalysis is an emerging technique valuable for water and air purification which offer the advantage of destroying the pollutants to degrade or transform into less harmful substances. However, heterogeneous photocatalysis is still in the research stage as some inherent important problems remain for efficient application. In this sense, fundamental research is still needed in order to improve the photocatalyst performance, increase the low photon efficiencies, achieve higher overall rates and decrease conversion times.

Titanium dioxide is widely used as a semiconductor photocatalyst because of its long-term stability, no toxicity and good photocatalytic activity [1]. However, there is still a problem that photocatalytic efficiency is not high since TiO_2 is active only under ultraviolet (UV) light because of its wide band gap ~3.2 eV and recombination of photogenerated electron–hole pairs results low photo quantum efficiency. The effective separateness of electron–hole pairs, therefore, is one of the important subjects for the increased utility of TiO_2 as a photocatalyst. In recent years, impurity doping has been widely performed by chemical synthesis and other methods in order to improve photoactivity [2]. Because transition metal elements have many valences and trace transition metal ions doped in the TiO_2 matrix can be superficial potential trap of photogenerated electron–hole pairs, then lengthen the lifetime of electrons and holes and increase photocatalytic activity.

Karakitsou and Verykios [3] showed that doping with cations having a valence higher than +4 can increase the photoactivity, whereas Mu et al. [4] reported that doping with trivalent or pentavalent metal ions was detrimental to the photoactivity even in the UV region. Furthermore, according to a systematic study on the photoactivity and transient absorption spectra of quantum-sized TiO_2 doped with 21 different metals the energy level and d-electron configuration of the dopants were found to govern the photoelectrochemical process in TiO_2 [5]. Even though the effects of metal doping on the activity of TiO_2 have been a frequent topic of investigation, it remains difficult to make unifiable conclusion on the effects of doping on photoactivities of TiO_2.

In these previous experimental investigations, impurities were mostly distributed uniformly in the TiO_2. Based on these previous experimental investigations, our group has expended our interesting in investigating the effect of doping modes, especially in non-uniform doping, on photoactivity of TiO_2 recently. In our investigation, innovative catalysts, surface non-uniform doped TiO_2, bottom non-uniform doped TiO_2 films were prepared. Considering the structure property and no toxicity, we chose group VIB element Mo

* Corresponding author. Tel.: +86-13535199508; fax: +86-2087057302.
E-mail address: lixj@ms.giec.ac.cn (X.-j. Li).
[1] Master of Science student. E-mail address: yangying300@sina.com (Y. Yang).

1010-6030/$ – see front matter © 2004 Elsevier B.V. All rights reserved.
doi:10.1016/j.jphotochem.2004.02.008

to modify TiO_2 and investigated the effects of doping mode and doping concentration on the photocatalytic activities of Mo^{6+}-doped TiO_2 films.

2. Experiments

2.1. Preparation of pure TiO_2 and Mo/TiO_2 films

Precursor solutions for TiO_2 films were prepared by the following method [6,7]: 68 ml tetrabutylorthotitanate and 16.5 ml diethanolamine were dissolved in 210 ml ethanol, then stirred vigorously for 1 h at room temperature (solution A), a mixture of 3.6 ml water and 100 ml ethanol (solution B) was added dropwise into the solution A with a burette, under stirring. The resultant alkoxide solution was left standing at room temperature for 2 h for hydrolysis reaction, resulting in the TiO_2 sol.

Soda lime glass (SLG, 35 mm × 200 mm × 2 mm) precoated with a SiO_2 layer according to the literature [8] was used as the substrates. The results showed that the catalytic activity of TiO_2-coated SiO_2/SLG was higher than that of TiO_2 films coated on bare SLG. The reason is that SiO_2 layers formed on the soda-lime glass effectively retarded sodium and calcium diffusion into nascent TiO_2 films.

The TiO_2 films formed on the substrates were prepared from the TiO_2 sol solution by dipping–withdrawing in an ambient atmosphere, then heat-treated at 500 °C for 1 h in air using an electric oven. The withdrawal speed was 2 mm/s. The thickness of the TiO_2 films was adjusted by repeating the above cycle.

For the preparation of doped titania film, the procedure was performed as the above besides that the respective amount of molybdenum nitrate from 0.3 to 1.5 at.% was dissolved in the solution B. TiO_2 can be doped by Mo in different modes signed as T, TM, MT, M representing pure TiO_2, surface non-uniform doped TiO_2, bottom non-uniform doped TiO_2, uniform doped TiO_2, respectively, which were describing in Table 1.

2.2. Characterization

The thickness of TiO_2 films was observed using scanning electron microscopy (SEM; type JSM-5600LV) with an accelerating voltage of 25 kV. Crystallinity of the TiO_2 films was determined by X-ray diffraction (XRD) using an diffractometer (type D/MAX-IIIA) with Cu Kα radiation. The accelerating voltage and the applied current were 30 kV and 30 mA, respectively. Spectroscopic analyses of TiO_2 films are performed by a UV-3010 UV-Vis spectrophotometer.

Table 1
The doping modes of TiO_2

Sample	Composing		
T	Two layers SiO_2-sol	Four layers TiO_2-sol	Four layers TiO_2-sol
TM	Two layers SiO_2-sol	Four layers TiO_2-sol	Four layers Mo/TiO_2-sol
MT	Two layers SiO_2-sol	Four layers Mo/TiO_2-sol	Four layers TiO_2-sol
M	Two layers SiO_2-sol	Four layers Mo/TiO_2-sol	Four layers Mo/TiO_2-sol

2.3. Photocatalytic activity verification

TiO_2 films are settled in a vessel ($\Phi = 70$ mm) in which 400 ml aqueous methyl orange with a concentration of 10 mg/l were added. A high-pressure mercury lamp (125 W, $\lambda_p = 365$ nm) is used as a light source. The vessel is immersed in a cooling bath in order to obtain a constant temperature. The solution is bubbled with air during irradiation. The concentration of aqueous methyl orange is determined with a UV-Vis spectrophotometer by measuring at 464 nm, the absorbance of the solution fetched every 10 min.

The photocatalytic decolorization of methyl orange is a pseudo-first order reaction and its kinetics may be expressed as $\ln(c_0/c) = K_{obs}t_{illum}$, where K_{obs} is the apparent reaction rate constant, t_{illum} the reaction time, and c_0 and c are the initial concentration and the reaction concentration of methyl orange, respectively.

2.4. Electrochemistry experiments

2.4.1. Preparation of film electrode

Titanium sheets (purity > 99.7%, 1.5 mm thick, 15 mm × 15 mm) was polished with $0^{\#}$ and $8^{\#}$ emery paper carefully washed with acetone, ethanol and distilled water in turn. The titanium oxide film electrode was made by dipping–withdrawing method as the above procedure (no SiO_2 layer). Then, the film sheet was linked to a lead and covered with epoxy resin except the working surface.

2.4.2. Electrochemistry test

Electrochemistry test was performed in three electrodes system made of quartz cells linked with CHI660 electrochemical station, as Fig. 1 showed. Film electrode(area 1.5 cm × 1.5 cm) served as the working electrode (WE); a platinum sheet (area 2 cm × 2 cm) and the saturation calomel electrode (SCE) served as the counter electrode (CE) and the reference electrode, respectively. The electrolyte was 0.5 mol/l Na_2SO_4 aqueous solution what were prepared by

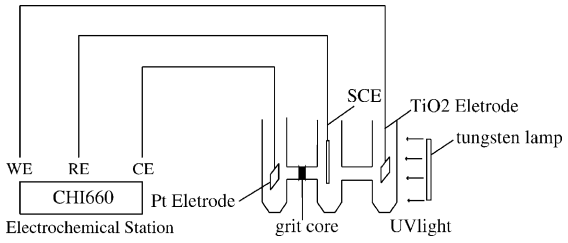

Fig. 1. Schematic diagram of reactor.

analytical reagents and distilled water. Photo electrochemical test was under tungsten lamp (5 W, $\lambda_p = 365$ nm). All the tests were kept at room temperature.

3. Results and discussion

3.1. Results and analysis

3.1.1. Film thickness

The thickness was measured using scanning electron microscopy by backward scatter technique after TiO_2 films cross-section was sprayed gold film in vacuum plating instrument. Fig. 2 showed SEM micrograph of TiO_2 film cross-section after dipping–withdrawing once and the thickness of one layer is about 30 nm. In the experiment, the films were prepared by dipping–withdrawing eight times, so the thickness was 240 nm or so.

3.1.2. XRD results

Fig. 3 shows XRD spectra of films of TiO_2 doped with Mo under different concentrations, which was treated smoothly.

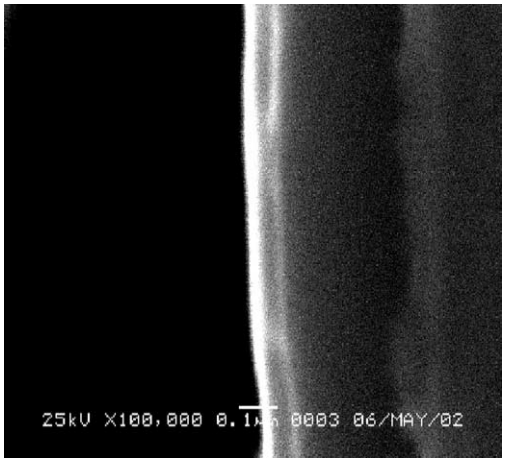

Fig. 2. SEM micrograph of TiO_2 films cross-section.

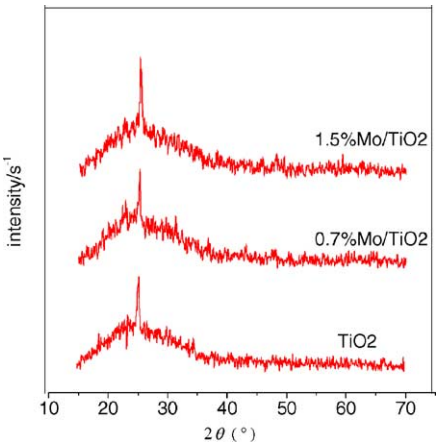

Fig. 3. The XRD spectra of TiO_2 and Mo/TiO_2 films.

Table 2
The lattice spacing of photocatalysts with different concentration of Mo

Samples	*d*-Value
TiO_2	3.526
Mo/TiO_2 (0.5%)	3.525
Mo/TiO_2 (0.7%)	3.523
Mo/TiO_2 (1%)	3.520
Mo/TiO_2 (1.5%)	3.517

The background of spectra is from glass substrate and the photocatalysts were in the form of anatase.

Table 2 showed the lattice spacing of photocatalysts with different concentration of Mo. As the concentration of Mo increasing, the lattice spacing decreased, according to Vegard law [9]: the lattice constant of solid solution increased with increasing solute concentration when the radius of solute atom is bigger than that of solvent atom, and it was reverse when the radius of solute atom is smaller than that of solvent atom.

3.1.3. Photocatalytic activity

Fig. 4 shows the relationship between methyl orange degradation rate and doping mode. It was clearly seen that the photocatalytic activity of MT was better than that of T, and TM and M mode were worse than T.

Fig. 5 shows the relationship between apparent first-order rate constant and the doped MoO_3 concentration (prepared by MT mode). It was found that the more doped MoO_3, the more activity, and the activity maximized at 1 at.% doped MoO_3 concentration, then the more doped MoO_3, the less activity.

3.1.4. UV-Vis transmittance spectra

Fig. 6 shows the UV-Vis transmittance spectra for the films of TiO_2 with different Mo-doping concentration. The absorption edge of the doped TiO_2 is observed at a longer wavelength range than that of the pure TiO_2. The absorption of visible light enhance along with the impurity concentration. The absorption of light maximized at 1 at.%. But the absorption edge is at a shorter wavelength range than that of the pure TiO_2 films as the Mo concentration was above

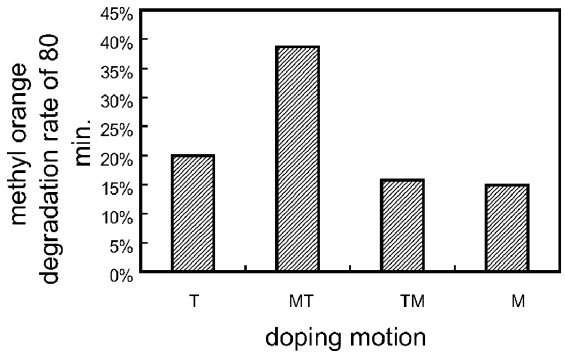

Fig. 4. Plot of methyl orange degradation rate vs. doping mode.

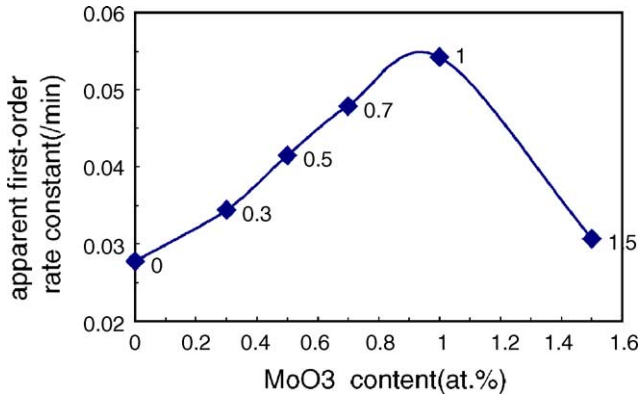

Fig. 5. The relationship between apparent first-order rate constant and MoO_3 concentration.

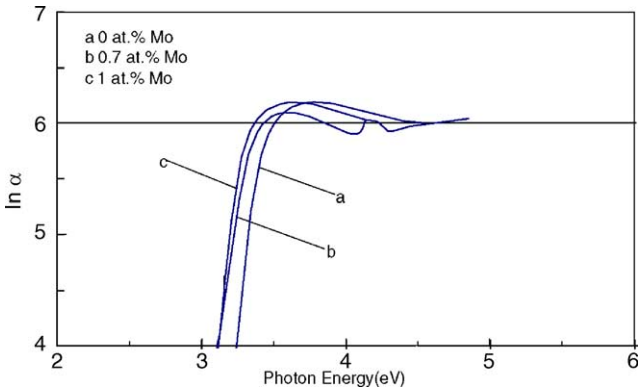

Fig. 7. Plot of ln α vs. photon energy.

1 at.%. This is consistent with the above activity results. This could be explained that the lattice cycle potential field was disarranged with Mo^{6+}-doping and brought the impurity level in the band gap near the bottom of the conduction bands [10], so the photon energy needed when electrons jumped across the energy gap into the impurity band decreased and the catalyst showed "red shift". As the Mo concentration increased, the absorption of light showed "blue shift", the detailed reason was needed further studying.

Fig. 7 showed the bandgap energy of TiO_2 with different Mo-doping concentration. According to the literature, the natural logarithm of the absorption coefficient α was recalculated to determine E_g at ln $a = 6$ [11]. This method of data analysis is common practice in solid-state sciences. It indicated that bandgap energy of 1 and 0.7 at.% Mo/TiO_2 were 3.35 and 3.39 eV and lessened compared with pure TiO_2 (3.42 eV, according to the literature [12]).

3.1.5. Electrochemical impedance spectroscopy

EIS Nyquist was used to study the electrochemical impedance spectroscopy characterize of Mo/TiO_2 film electrodes with different doping mode and different doping concentration (all prepared by MT mode) obtained with illumination. The amplitude was 0.2 V, signal frequency range is 10^{-2} to 10^5 Hz. The radius of circular arc in EIS Nyquist plots was corresponding to the charge transfer resistance and the separate efficiency of the electron–hole pair [13]. Fig. 8 shows EIS Nyquist plots of Mo/TiO_2 film electrodes with different doping mode obtained with illumination and it indicated that the radius of circular arc varied with following sequence: $R_{MT} < R_T < R_M < R_{TM}$, viz. the charge transfer resistance of the film by MT mode was the least and the separate efficiency of the electron–hole pair was the best, which corresponded to the photocatalytic experiment result.

Fig. 9 shows EIS Nyquist plots of Mo/TiO_2 film electrodes with different doping concentration obtained with illumination. It can been seen that the charge transfer resistance decreased with increasing Mo concentration and maximized at 1 at.%, but it increased as the Mo concentration was above 1 at.%, viz. the separate efficiency of the electron–hole pair was the best at 1 at.% doping concentration. This maybe resulted from that Mo^{6+} can capture the photogenerated carriers and prolonged the carrier lifetime and quickened carrier separating. As the doping

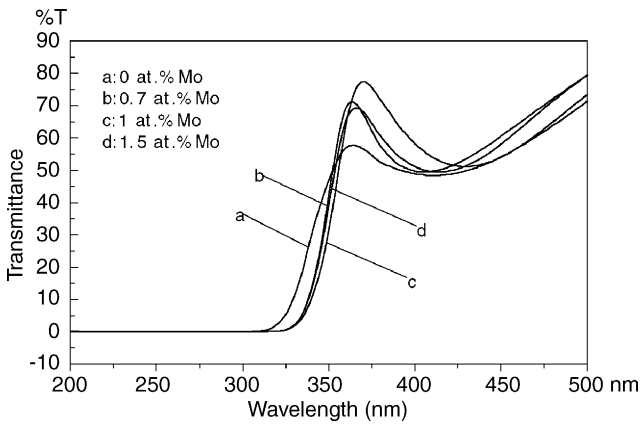

Fig. 6. The UV-Vis transmittance spectra as a function of wavelength for Mo/TiO_2 films.

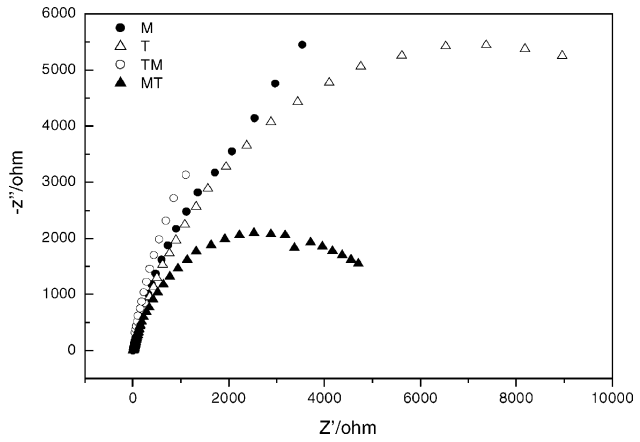

Fig. 8. EIS Nyquist plots of Mo/TiO_2 film electrodes under various doping mode obtained with illumination.

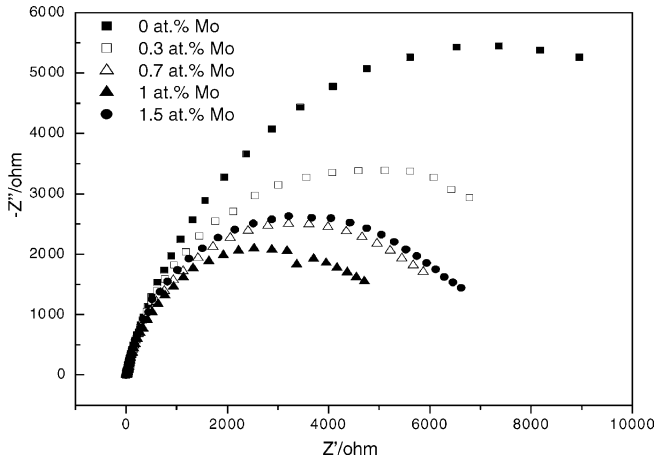

Fig. 9. EIS Nyquist plots of Mo/TiO_2 film electrodes under various doping concentration obtained with illumination.

concentration increased overly, the captured-carrier recombined its counter generated by later photon and the capture trap became carrier recombination center [14].

3.2. Discussion

3.2.1. Doping mode analysis

Pure titania is n-type semiconductor because of the presence of oxide vacancies ($V_{\ddot{O}}$). A defect was created in the crystal when Mo^{6+} substituted Ti^{4+} in the lattice. In the Kroger-Vink notation, this is written as follows [15,16]:

$$MoO_3 \rightarrow Mo_{\ddot{T}i} + 2e' + 2O_0^x + \tfrac{1}{2}O_2 \uparrow \quad (1)$$

After Ti^{4+} was substituted, the electron concentration increased because of charge equilibrium. Mo^{6+} became the electron donor, the Fermi level in band gap moved upwards and the width of band gap narrowed compared with pure TiO_2.

With illumination, for Mo/TiO_2 films doped by MT mode, Fermi level of TiO_2 in the layer (designated as bottom layer) prepared from Mo/TiO_2 sol is higher than that in the layer (designated as surface layer) prepared from TiO_2 sol, thus electron concentration in bottom layer is higher than that in surface layer. So electrons in bottom layer will diffuse to surface layer, in the same time, holes in surface layer will diffuse to bottom layer. As a result, positive–negative space-charge layer will be formed, and then the electric field from bottom layer to surface layer will baffle e^-–h^+ diffusion to each other. When carriers diffusion reaches equilibrium, Fermi level in the system is in the same level, and band near interface bends and form carrier barrier, and this situation is similar to the heterogeneous junction [17], which retards recombination of electron–hole pairs. Fig. 10 showed Energy levels schematic diagrams of MT films and band bending.

As surface holes are consumed by oxidation reaction, holes near interface in bottom layer will move to surface

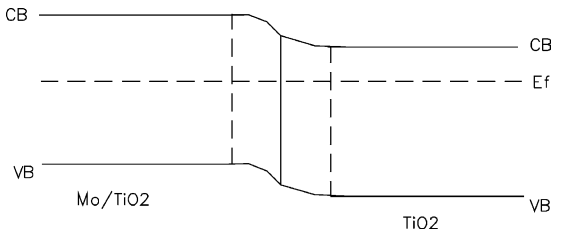

Fig. 10. Energy levels schematic diagrams of MT films and band bending.

layer in the effect of the electric field. So hole concentration in surface layer increases and photocatalytic activity enhances. As to Mo/TiO_2 films doped by M mode, it cannot form carrier barrier, and may be electron–hole recombination centers. For Mo/TiO_2 films doped by TM mode, it will form the reverse electric field in the interface. When surface holes are consumed by oxidation reaction, owing to the presence of the reverse field, holes in bottom layer cannot move to surface, so surface holes are fewer than those in T mode. Because holes are major factor in the photocatalytic reaction, the photocatalytic activity is lower than pure TiO_2 under surface Mo^{6+}-doped and bulk Mo^{6+}-doped modes.

In addition, the photocatalytic reaction is surface reaction. When there are many dopants in surface of TiO_2 films, on the one hand they cannot have photocatalytic activity and join photocatalytic reaction; on the other hand they capture electrons and holes on the surface layer and then maybe counteract photocatalytic reaction and become surface electron–hole recombination center. So the best doping mode is impurity doped in the bottom of the films [14]. The experiment result shows that the photocatalytic activity is lower than pure TiO_2 when impurity is introduced on the surface, such as surface Mo^{6+}-doped and bulk Mo^{6+}-doped modes; the photocatalytic activity increased obviously when impurity is introduced on the bottom, such as bottom Mo^{6+}-doped modes.

3.2.2. Doping concentration analysis

The oxidation–reduction potential of Mo^{6+}/Mo^{5+} is 0.4 eV and that of Ti^{4+}/Ti^{3+} is 0.1 eV [18], so Mo^{6+} can capture photogenerated electrons more easily, thus can avail separate of carriers and enhance photocatalytic activity. The suitable amount dopants can capture photogenerated electrons and decrease the rate of recombination of electron–hole and accelerate photocatalytic reaction.

As the concentration of dopant increases, electron–hole pairs captured overcome barrier and recombine. However, at a certain level of dopant, the rate of recombination starts dominating the reaction [19]:

$$K_{\text{recomb}} \propto \exp\left(\frac{-2R}{a_0}\right) \quad (2)$$

Where K_{recomb} is the rate of recombination, R the distance between the trap site of e^- and h^+ and a_0 is the hydrogenic radius of the wave function for the charge carrier. It can seen

from (2), as above optimal concentration, with reduction of the distance between the trap site, the rate of recombination increase exponentially, so photocatalytic activity decrease.

On the other hand, when the dopants are excessive, Mo^{6+} cannot enter the TiO_2 lattice but cover on the surface of TiO_2 in MO_3 form, and form heterogeneity junction [20]. The valence bands and conduction bands of two crystals maybe link paratactically and charge capture centers maybe become recombination center, so photocatalytic activity reduce.

4. Conclusion

The results shows that the best doping mode is Mo^{6+}-doped on bottom layer and the photocatalytic activity is lower than pure TiO_2 under surface Mo^{6+}-doped and bulk Mo^{6+}-doped modes. It is maybe forming barrier of carrier under bottom Mo^{6+}-doped mode and then retard the (e^-–h^+) pair recombination. With the doping concentration increasing, the charge transfer resistance of interfacial decreased and the photodegradation efficiency of methyl orange increased and the absorption edge was extended; as doping concentration was above 1 at.%, each was reverse situation, viz. the photocatalytic activity was best in 1 at.% doping concentration.

Acknowledgements

The authors are grateful for financial support from Guangdong Natural Science Foundation (Project No. 010873) and the department of Science and Technology of Guangdong Province (Project No. 2002C31621).

References

[1] O. Legrini, E. Oliveros, A.M. Braun, Chem. Rev. 2 (1993) 671.
[2] H. Yamashita, Y. Ichihashi, M. Takeuchi, S. Kishiguchi, M. Anpo, J. Synchrotron Rad. 6 (1999) 451.
[3] K.E. Karakitsou, X.E. Verykios, J. Phys. Chem. 97 (1993) 1184.
[4] W. Mu, J.M. Herrmann, P. Pichat, Catal. Lett. 3 (1989) 73.
[5] W. Choi, A. Termin, M.R. Hoffmann, Phys. Chem. 98 (1994) 13669.
[6] K. Kato, A. Tsuzuki, Y. Torii, H. Taoda, T. Kato, Y. Butsugan, Mater. Sci. 30 (1995) 837.
[7] X.-J. Li, F.-B. Li, G.-B. Gu, Chin. J. Nonferrous Met. 6 (2001) 971.
[8] A. Duran, J.M. Fernandez Navarro, P. Casariego, A. Joglar, J. Non-Cryst. Solids 82 (1986) 391.
[9] J. Friedel, Phil. Mag. 46 (1995) 514.
[10] K. Huang, R.-Q. Han, Solid Physics, Advanced Education Press, Beijing, 1988.
[11] M.S. Jeon, et al., Appl. Surf. Sci. 165 (2000) 209.
[12] C. Kormann, D.W. Bahnemann, M.R. Hoffmann, et al., Phys. Chem. 92 (1988) 5196.
[13] H. Liu, M. Wu, H.-J. Wu, Acta Phys. Chem. Sin. 3 (2001) 286.
[14] X.-Y. Yu, J.-J. Cheng, J. Inorg. Mater. 4 (2001) 742.
[15] Y.-Q. Wang, L. Zhang, H.-M. Cheng, Chem. J. Chin. Univ. 6 (2000) 958.
[16] D.V. Ragone, Thermodynamics and Kinetics of Materials, Wiley, Canada, 1995.
[17] K. Huang, X.-D. Xie, Semiconductor Physics, Science Press, Beijing, 1958.
[18] X.-T. Peng, Inorganic Chemistry, Advanced Education Press, Beijing, 1996.
[19] P.-Y. Zhang, G. Yu, Zh.-P. Jiang, Adv. Environ. Sci. 3 (1997) 1.
[20] Sh.-X. Zhan, Sh.-H. Fan, Z.-H. Lin, Acta Sci. Nat. Univ. Sunyatseni 2 (2001) 125.